APEM journal
Advances in Production Engineering & Management
Volume 15 | Number 4 | December 2020 | pp 441–452
https://doi.org/10.14743/apem2020.4.377
ISSN 1854-6250
Journal home: apem-journal.org
Original scientific paper

Effect of glass and carbon fibres on the compressive and flexural strength of the polymer concrete composite

Petruška, O.[a], Zajac, J.[a], Dupláková, D.[a,*], Simkulet, V.[a], Duplák, J.[a], Botko, F.[a]

[a]Technical University of Košice, Faculty of Manufacturing Technologies with a seat in Prešov, Institue of Advanced Technologies, Prešov, Slovak Republic

ABSTRACT

This article is focused on testing the mechanical properties of polymer concrete testing samples. After a thorough literature search, the basic conditions of the research were determined and under the standards, three types of samples of special new concrete mixtures were created as a building element for special CNC machines. The samples were subjected to the research of the influence of used fillers, binders and additives on their properties. Testing was carried out in a certified laboratory and included checking the dimensions of the test bodies, weighing on the calibrated weight, determining the volumetric weight, determining the maximum load of the testing samples using special devices and then determining the compressive strength, or flexural tensile strength according to the relevant formulas. The final part of the testing also examined the morphology and mapping of the chemical composition with a focus on carbon, oxygen and aluminum using an electron microscope. The obtained results clearly show an increase in tensile and compressive strength using dispersed carbon fibre reinforcement of approximately 4 MPa. The conclusion of the article provides an overall summary of the results obtained and a summary of the features.

ARTICLE INFO

Keywords:
Concrete composite;
Polymer concrete;
Compressive strength;
Flexural strength;
Glass fibres;
Carbon fibres

**Corresponding author:*
darina.duplakova@tuke.sk
(Dupláková, D.)

Article history:
Received 21 January 2019
Revised 30 November 2020
Accepted 3 December 2020

1. Introduction

The structures of machines used for machining have to correspond to the increasing performance and dynamic parameters, namely the stiffness and damping parameter. At present, materials such as steels and cast irons are conventionally used in these constructions to meet the rigidity requirements, but they are characterized by low damping [1-3]. If the machine has a high dynamic, these conventionally used materials are not able to adequately absorb the impact from the drive. The impacts make the machine vibrations, which are perceived as a negative impact throughout the production process. One option to eliminate the vibrations of machines made of steel or cast iron is to replace the construction materials [4-5]. One of the possible materials that the existing problem could eliminate is polymer concrete. This material is essentially a composite material [6-7] and it is characterized by the synergistic effect, which means that the value of the properties of the resulting composite material is higher than the sum of the properties for each component separately. This special material is a combination of binder, filler and other suitable admixtures. The particular ingredients achieve the desired properties for a particular use. Since polymer concrete is composed of natural materials which can be recycled at the end of the casting life, this material becomes a modern non-conventional material [8-10].

Many experts are dedicated to the research of polymer concrete mixtures. The study of microstructure and mechanical properties with the creation of the quantitative characterization methodology for concrete containing polymeric fibres was discussed by a team of authors Trofimov *et al.* [11]. Authors Tanyilizi and Asilturk in their research paid attention to the strength properties of polymers containing phosphazene during the exposure to high temperatures. This study utilized the Taguchi L-25 method (5 (5)), which reduced the number of experiments to find parameters influencing the experimental results. Research has shown that polymer concrete can favourably effect on the structure of buildings that are exposed to high temperatures under determined conditions [12]. Strength analysis and determination of deformation characteristics of methyl methacrylate modified vinyl ester were studied in 2018. In this study, attention was paid to curing temperatures as the test variable. After the research, it was found that the increased modulus of MMA decreases the modulus of elasticity and the heat of solidification [13]. The research by Simsek and Uygunoglu was focused on mechanical properties, workability and thermal properties of polymers, namely polycarbonate, thermoplastic polyurethane and polybutylene terephthalate mixed concrete. During the research, they were selected and optimized special properties by using full factorial design through Minitab software [14]. In the current research, attention was also paid to the analysis of the increase in elasticity of epoxy polymer concrete with short natural fibres, namely sisal fibres and ramie fibres [15]. In the field of civil engineering, it was researched flexural efficiency in the polymer concrete with the basalt fibre. The testing evaluated the compression and flexural properties, cracks, stresses and disturbances. Based on the experiments carried out, it was developed the guidelines for sea-sand concrete beams with basalt fibre bar-reinforced [16]. In the Materials Journal, there was presented research focused on the creation and evaluation of microstructure, mechanical and physical properties of recycled glass aggregate additive implemented in polymer concrete. Recycled glass fractions were added to the individual mixtures, with the most appropriate physical and mechanical properties being achieved by applying a 50 % recycle deposit to the polymer concrete mixture [17]. The thermal and mechanical properties of the glass-fibre polymer concrete composite were also described by Schmitt *et al*. This paper was focused on the experimental investigation of sandwich panels made of polymer-fibre material with glass fibre adhesion and polystyrene insulation layer. The panels were subjected to extreme experimental conditions, with a significant change in the insulation layer resulting in a reduction in total stiffness and load capacity [18]. The issue of the influence of the basalt, ash and silica sand on the mechanical properties of the polymer-concrete material was also addressed in the paper published in the Bulletin of Materials Science. The paper describes the study of the production of these polymers and the optimization of the weight percent of the epoxide resin, silicon sand, ultra-fine ash and basalt [19]. A team of authors Burlacu *et al*. in their research focused on testing the polymer concrete made from polystyrene granules. During the study, the impact of the granules on the mixture density, compressive strength, bending strength and tensile strength was analysed. The results obtained showed a decrease in mechanical properties by increasing the substitution dose of polystyrene granules [20]. Research of the production and assessment of physical, mechanical and thermal properties of various mixtures were discussed by many authors such as [21-31].

As can be seen in the previous survey of the research, the research of the properties of polymer concrete is currently carried out by a large number of experts. However, as can be seen from the above-mentioned survey, these studies are rather focused on building engineering and not on the field of research into the construction of machinery and equipment. The present paper provides a preview of the mechanical properties of the mixtures with a focus on the field of engineering - specifically on the field of construction of machines. The main contribution of the article lies in the determination and presentation of the obtained properties of newly created materials, which will serve as an elementary building element in the design solution for special CNC machines used for machining parts using DMLS technology.

2. Material and methods

Twelve test samples were produced, representing 3 types of the composition of the mixture. These test samples were tested for compressive strength and flexural tensile strength. According to STN EN 12390-3, at least 3 test bodies of the same composition have to be tested to make the measurement (experiment) statistically significant. For this reason, 3 test bodies of each type of composition were produced. This is a total of 9 test samples that have been tested for compressive strength. Three further test samples, one of each kind, were tested for flexural tensile strength. The test samples according to STN EN 12390-1 have the shape of a cube, cylinder and prism. This standard includes standardized dimensions, tolerances and types of moulds. For the compression strength tests, they have produced test cubes with 150×150×150 mm dimensions. For tensile strength tests, prism-shaped test pieces of 100×100×500 mm were produced.
Both organic (natural) and inorganic (artificial) fillers were used as testing samples. The organic fillers included silicate sand and gravel with the parameters shown in Table 1.

The 6 mm glass and 3 mm carbon fibres in the form of dispersed reinforcement were used. The matrix was the epoxy resin CHS-EPOXY 324 and hardener TELATIT 0492. The properties of the resin and hardener used are described in Table 2.

The advantages of the binder system (matrix) are excellent adhesion, high thermal and chemical resistance and high strength. Tables 3 and 4 illustrate the properties of the binder system used during the production and / cured system properties measured after 7 days hardening at 23 °C and hardening for 2 hours at 120 °C.

The system resists diluting mineral acids (hydrochloric acid 10 %, nitric 10 %, sulfur 30 %), an alkaline solution (sodium hydroxide 40 %, ammonia 10 %), water, gasoline, oil and diesel oil. It does not resist organic acids (acetic acid 5 %, milk 10 %).

Table 1 Organic fillers

Name	Type	Fraction size (mm)
STJ 25	Silica powder	0.06-0.31
ST06/12	Silica Sand	0.63-1.2
ST PBT 4	Silica grit	2-4

Table 2 Properties of CHS-EPOXY 324 resin and TELATIT 0492 hardener

Name	Property	Value	Unit
CHS-EPOXY 324	Viscosity – at temperature 25 °C	20-60	Pa·s
	Epoxy index	3-3.4	mol·kg^{-1}
	Epoxy mass equivalent	294-333	g·mol^{-1}
	Colour	maximum 300	j·Hazen
TELATIT 0492	Viscosity at temperature 23 °C	15-30	mPa·s
	Density at temperature 23 °C	0.93-0.96	g·cm^{-3}
	Aminic equivalent	550-600	mg KOH·g^{-1}
	Hydrogen equivalent	minimum 49	g·mol^{-1}
	Colour	maximum 3	Gardner

Table 3 Properties of bending and hardening system during the production

Bending system	Max. exotherm	Jellify time	Processability time
	(°C)	(hod)	(min)
CHS-EPOXY 324/TELATIT 0492	118	3	50-70
Hardening system	Modulus of rigidity	Strength in flaking	Tensibility
	(MPa)	(N·cm^{-1})	(%)
CHS-EPOXY 324/TELATIT 0492	25	14	3

Table 4 The ratios of the ingredients in the test samples

Testing samples No. 0623-0001, No. 0623-0002, No. 0623-0003 and No. 0623-0010		
Filler 70 %	48 %	ST PBT 4
	28 %	06/12
	18 %	STJ 25
	6 %	Carbon fibre (3 mm)
Binder 30 %	100 portions	CHS-EPOXY 324
	16 portions	TELATIT 0492
Testing samples No. 0623-0004, No. 0623-0005, No. 0623-0006 and No. 0623-0011		
Filler 70 %	48 %	ST PBT 4
	28 %	06/12
	18 %	STJ 25
	6 %	Glass fibre (6 mm)
Binder 30 %	100 portions	CHS-EPOXY 324
	16 portions	TELATIT 0492
Testing samples No. 0623-0007, No. 0623-0008, No. 0623-0009 and 0623-0012		
Filler 70 %	50 %	ST PBT 4
	30 %	06/12
	20 %	STJ 25
Binder 30 %	100 portions	CHS-EPOXY 324
	16 portions	TELATIT 0492

3. Experimental setup, results and discussion

Plastic moulds of standardized dimensions were used for casting, and each type of composition was cast from a single production batch to ensure complete compliance of the individual components in all test samples. First, the batch processing and mixing of the fillings was performed to ensure that the components were evenly distributed throughout the volume. Thereafter, batch processing and mixing of CHS-EPOXY 324 epoxy resin and TELATIT 0492 hardener were performed using a hand-held electric blender for 3 minutes. Subsequently, the filler was added to the binder (the matrix) under constant mixing. This process lasted for another 5 minutes to completely lubricate the filler and ensure the best adhesion. Then, casting into plastic moulds and vibrating the moulds on the vibration table was done to optimize compaction and removal of air bubbles. It took 2 minutes. Subsequently, the moulds were filled onto the work table and after 24 hours the polymers were cast from these moulds. Test assemblies were then stored in a curing room at 23 ± 1 °C with relative humidity 65 ± 5 % for 20 days.

Testing samples were tested by the Technical and Testing Institute in the accredited testing laboratory. The test samples were tested 20 days after the date of manufacture to have a hardening time of 15 days from the casting process. During the experiment, there were performed 9 compression strength tests and 3 flexural tensile tests. The room temperature was 19 ° C and the relative humidity was 60 %. Testing of test samples was carried out according to STN EN 12390-1. This standard defines, in particular, the possible shapes of the test samples, their standardized sizes and allowed variations in the length of the walls, perpendicularity and planarity. All test samples have passed shape and dimension control. Fig. 1 shows dimension measurement using a Mitutoyo ABSOLUTE AOS 500 calibrated digital scroll gauge. The device provides the measurement accuracy up to a measured length of a maximum 200 mm within ± 0.02 mm. The Mitutoyo ABSOLUTE AOS 500 was also used to measure the length of the prism, but a large measuring range, namely 0 mm to 600 mm, with a precision of ± 0.05 mm.

Fig. 1 Dimension inspection of the test sample

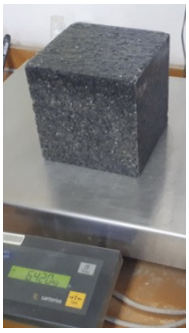

Fig. 2 Weighing of testing samples

Additionally, weighing the test samples (Fig. 2) and determining the volumetric weight – this part of the experiment was done according to the standard STN EN 12390-7. In the experiment, the method was realized by calculating the measured dimensions due to that dimension measurement was necessary for the previous part to check the test samples. From the measured dimensions, the volume of the test samples was calculated and then the weights were taken. This was done on a Sartorius®-EA150-FEG-l high-resolution digital calibrated scale. This device can weigh samples with a maximum weight of 150 kg, accuracy of weighing is within ± 5 g and has a weighing area made of galvanized steel measuring 500×400 mm.

Based on the determined volume of testing samples and measured weigh, the volumetric weight was calculated according to the formula:

$$D = \frac{m}{V} \tag{1}$$

where: D – the volumetric weight of testing sample (kg/m^3), m – weight of testing sample (kg), V – the volume of the testing sample (m^3).

The obtained results of volumetric weight are round of 10 according to standard STN EN 12390-7. In Table 5, there is presented the measured sizes, weight and volumetric weight of testing samples.

Table 5 Specification of testing samples

Sample	Sample number	Dimension			Weight (kg)	Volumetric weight (kg/m^3)
		Push area (mm)		Height (mm)		
Cube	0623-0001	150.8	150.1	150	6.420	1890
	0623-0002	152.1	150.1	150	6.630	1940
	0623-0003	151.9	150.0	150.0	6.470	1890
	0623-0004	151.5	150.0	150.1	6.320	1850
	0623-0005	150.1	150.7	150.6	6.380	1860
	0623-0006	152.7	150.1	150.0	6.355	1850
	0623-0007	151.6	149.8	149.9	6.560	1930
	0623-0008	152.0	150.1	150.2	6.570	1920
	0623-0009	151.9	150.2	150.0	6.625	1940
Prism		Width	Height	Length		
	0623-0010	101.2	100.3	499.6	9.430	1860
	0623-0011	102.5	100.4	499.8	9.435	1840
	0623-0012	102.6	100.2	500.0	9.985	1940

3.1 Execution of compression strength test, and obtained results

Then the compression strength was measured according to STN EN 12390-3. Testing was carried out on the CONTROLS, model: 50-C0050/HRD7 with a maximum load of 3000 kN, and machine weight 1140 kg which is shown in Fig. 3.

The testing sample was positioned on the lower pressing plate of the press machine so that the deviation from the centre was not more than ± 1 % of the length of the edge of the cube. The test sample was turned in such a way that the compressive force applied perpendicularly to the direction in which the polymer was placed into the mould, i.e. the top surface of the casting on the side. A constant test load rate of 0.6 MPa/s was then set. After the initial load, the sample was loaded according to a set speed until the maximum load was reached. According to the

Fig. 3 Compressive strength testing

standard, the movable upper pushing surface stops after reaching it, then rises to a zero position, and assesses whether the type of failure of the test piece complies with the standard. The standard image contains both satisfactory and unsatisfactory types of test sample breaks. The tested samples did not have a visible break as the test press automatically recorded the maximum load possible and returned to the initial position. Subsequently, the compressive strength of the test samples was determined according to the equation:

$$f_c = \frac{F}{A_C} \tag{2}$$

where: f_c – Compressive strength (MPa), F – total force at break (N), A_C – section of a testing sample (mm^2).

In Table 6, there is presented the results of compressive strength testing.

Table 6 Compressive strength for testing samples

Testing sample	Maximum pushing force (kN)	Compressive strength (MPa)		
		Calculated value	Round value ± U ($k = 2$)	Average value
0623-0001	1775.4	78.45	78.5 ± 0.9	
0623-0002	1829.0	80.10	80.1 ± 1.0	79.00
0623-0003	1787.8	78.44	78.4 ± 0.9	
0623-0004	1657.6	72.96	73.0 ± 0.9	
0623-0005	1705.3	74.68	74.7 ± 0.9	70.23
0623-0006	1442.7	62.97	63.0 ± 0.8	
0623-0007	1751.2	77.12	77.1 ± 0.9	
0623-0008	1719.7	75.37	75.4 ± 0.9	75.26
0623-0009	1673.1	73.35	73.3 ± 0.9	

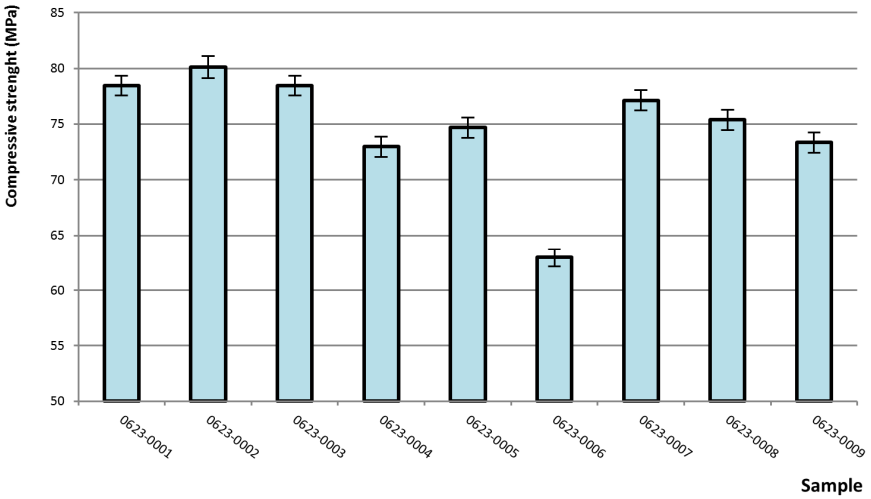

Fig. 4 Graphical representation of compressive strength for individual samples of polymer concrete mixture

Fig. 4 shows individual values of compressive strength of polymer concrete samples. As can be observed from figure values of compressive strength are in the range from 63 MPa to 85 MPa. Different types of reinforcement influence polymer concrete mechanical properties.

Fig. 5 shows comparison compressive strength for different mixtures of polymer concrete. As can be observed from the figure above the compressive strength of polymer concrete samples for the same reinforcement is in a very small interval. Highest compressive strength was measured for samples with short carbon fibre reinforcement. Also, good results for compressive strength testing were obtained for samples without fibre reinforcement. Values were slightly lower compared to carbon fibre reinforced samples. Samples prepared using glass fibre shows higher dispersity of compressive strength values. In this case, it can be stated that this type of reinforcement negatively influences the compressive strength of polymer concrete mixture.

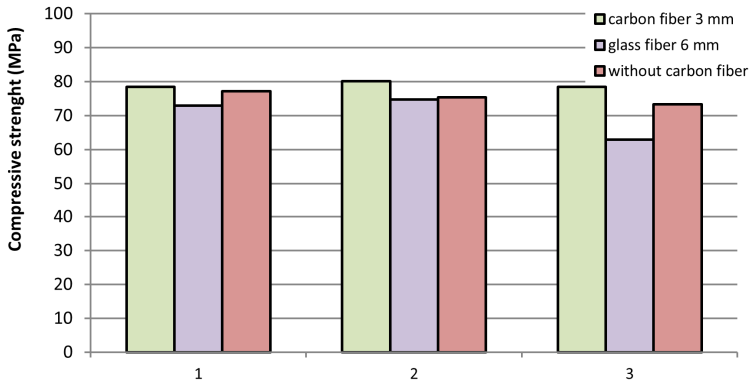

Fig. 5 Comparison of compressive strength of polymer concrete mixtures

3.2 Execution of flexural tensile test, and obtained results

In the second experiment, there was realised flexural strength according to EN 12390-5. Testing was executed by CONTROLS 50-C1201 machine which is shown in Fig. 6. This test machine has a special frame designed to minimize deformation at maximum pressure, resulting in high measurement accuracy. Technical parameters of the machine: maximum load 100 kN, maximum vertical distance 182 mm, maximum horizontal distance 720 mm, the distance between upper rollers 100 mm, 150 mm or 200 mm, the distance between bottom rollers adjustable from 50 mm to 900 mm, machine dimensions 950×1000×981 mm, and weight 175 kg.

Before the experiment, the spacing of the upper load rollers and the lower support rollers of steel with circular cross-sections and a diameter of 40 mm was set. The length of the rollers was 300 mm, so they met the test condition that they must protrude from the test sample at least 5 mm on both sides of the print area. They also met the requirements that they freely rotate around their axes and were moved in a perpendicular area to the longitudinal axis of the test sample. Roller surround was set according to the scheme presented in Fig. 7.

Fig. 6 Flexural strength testing

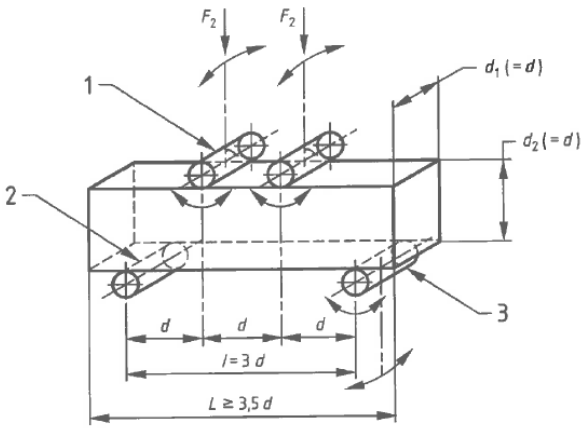

Fig. 7 Load layout scheme of testing sample

Fig. 8 Load layout scheme

Then, the sample was centrally positioned in the press machine by a longitudinal axis perpendicular to the longitudinal axes of the upper and lower rollers. The test body has been rotated so that the reference direction of loading is perpendicular to the direction in which the polymer was placed into the mould, i.e. the top surface of the casting on the side. A constant load rate of 0.05 MPa/s was then set. After the initial load, the sample was loaded at a set speed until the maximum load was reached. Achieving this boundary caused a transversal break of the test body, Fig. 8.

After the experiment, it was determined by the tensile strength at the bending of the test bodies according to the equation:

$$f_{cf} = \frac{F \cdot l}{d_1 \cdot d_2^2} \tag{3}$$

where: f_{cf} – flexural strength (MPa/s), F – maximum load (N), l – distance between supporting rollers (mm), d_1, d_2 – cross-section dimension of testing sample (mm).

In Table 7, there are presented the results of flexural strength testing.

Fig. 9 shows a comparison of flexural strength for samples prepared using carbon fibre reinforcement, glass fibre reinforcement and without fibre reinforcement. Highest flexural strength was observed for the sample prepared using carbon fibre reinforcement. Difference between the sample with glass fibre reinforcement and without reinforcement was 1 MPa.

Table 7 Flexural strength for testing samples

Testing sample	Maximum pushing force (kN)	Flexural strength (MPa)
		Round value ± U (k = 2)
0623-0010	83.99	24.8 ± 0.4
0623-0011	76.67	22.3 ± 0.4
0623-0012	72.18	21.0 ± 0.4

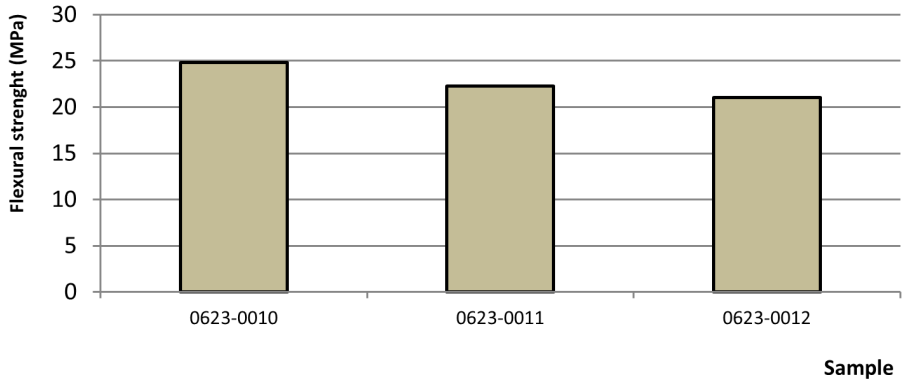

Fig. 9 Comparison of flexural strength of polymer concrete mixtures

3.3 Morphology of fracture area

The Tescan Mira 3 electron microscope observed for determination of the morphology of the fracture area. Samples for observation were carbon-cured to maintain the conductivity of the electron beam transition. Figs. 10, 11, and 12 show the observed samples of the polymer-composite composite at magnifications of 80×, 400×, and 2000×.

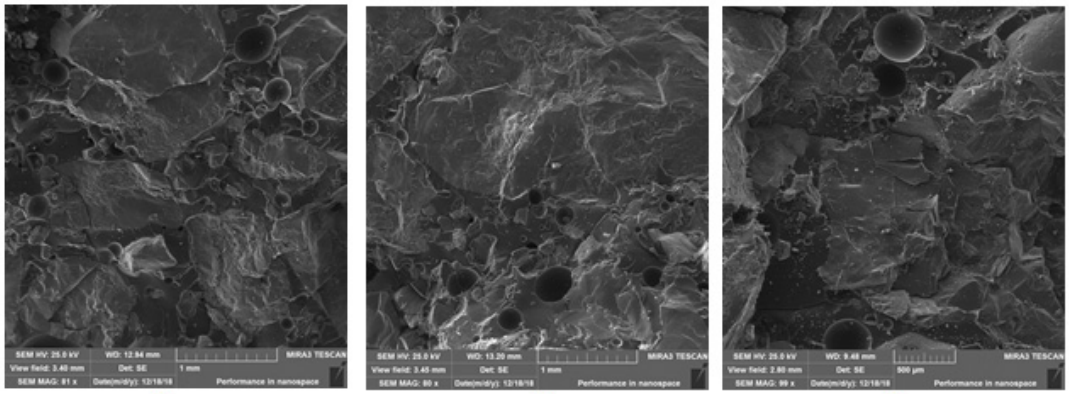

a) b) c)

Fig. 10 Polymer concrete composite with: a) sand, b) carbon fibres, c) glass fibers (magnification 80×)

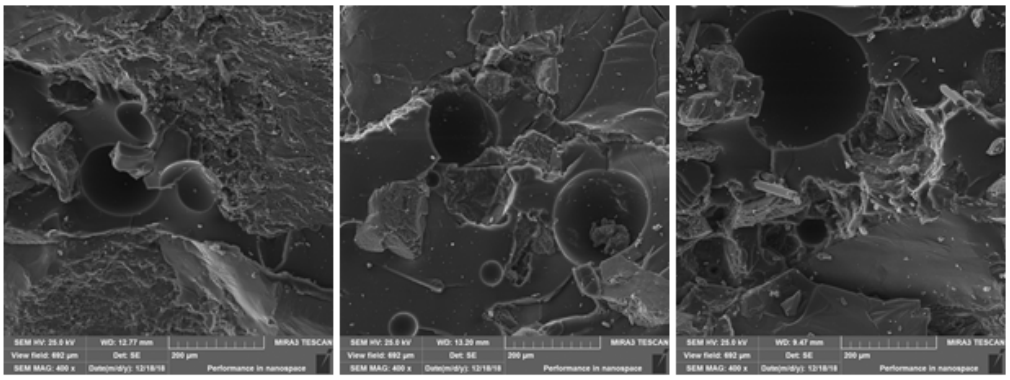

a) b) c)

Fig. 11 Polymer concrete composite with: a) sand, b) carbon fibres, c) glass fibers (magnification 400×)

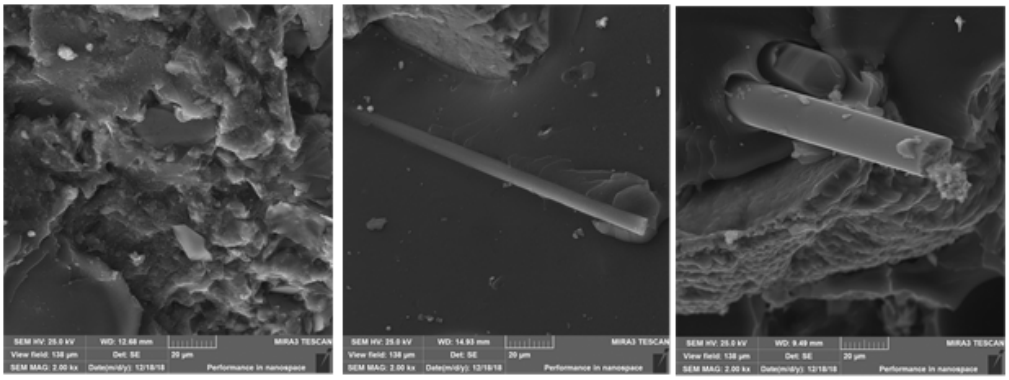

a) b) c)

Fig. 12 Polymer concrete composite with: a) sand, b) carbon fibres, c) glass fibers (magnification 2000×)

In the case of the second and third type samples, the reinforcing fibre used is visible at higher magnification. In both cases, the fracture area is visible; it is here to see the places of aggregate in various shapes (spherical and sponge-shaped). At a magnification of 400×, a hole in the resin is also visible, indicating the presence of air cavities in the polymerization process or by tearing of particles of aggregate. The reinforcing carbon fibres used are sufficiently coated with resin. In the case of the use of glass fibres, they were partly touching aggregates (Fig. 12c).

Observations also revealed the distribution of the material by mapping the chemical composition – carbon, oxygen, and aluminium. In the sample of the first type, silicon also showed us, suggesting the use of sand. With the same magnification observed, Fig. 13 shows a visible distribution of filler and binder. The binder of the resinous form is represented by a red colour containing the carbon component. The aggregate as filler contains oxygen, aluminium, and silicon, shown in blue and green below. Oxygen has a lower presence, suggesting an associated silicon and aluminium component in the form of SiO_2 and Al_2O_3.

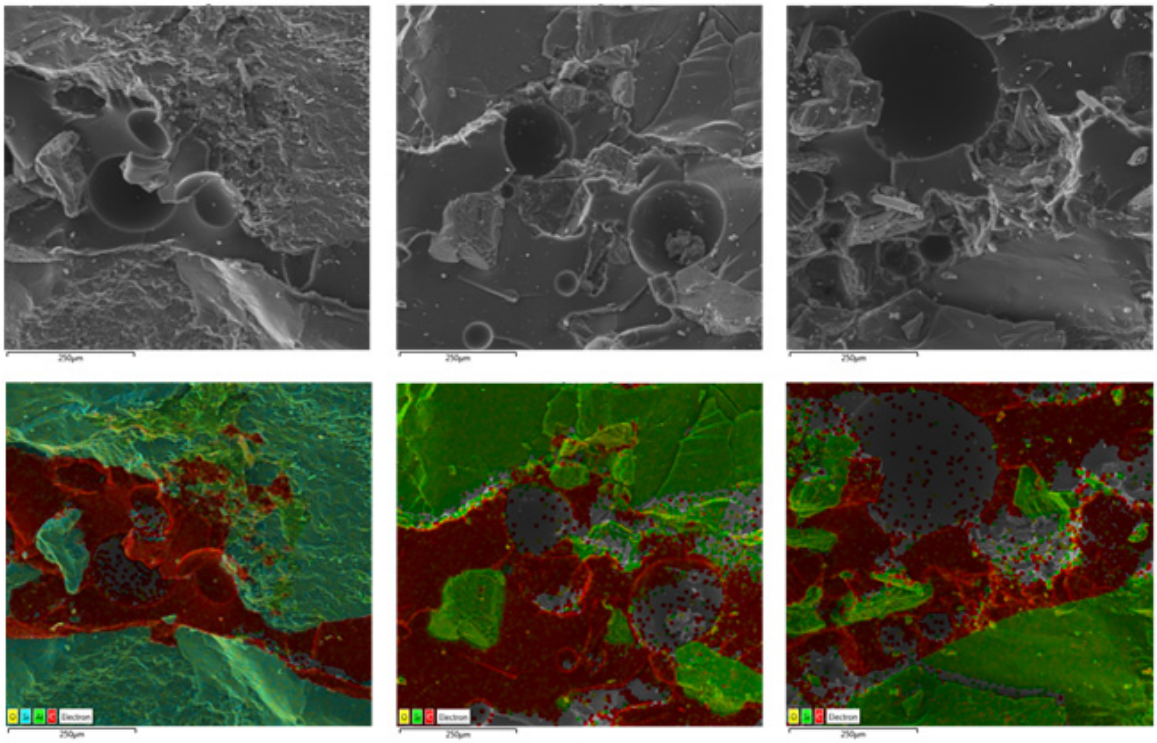

a) b) c)

Fig. 13 Polymer concrete composite with: a) sand, b) carbon fibres, c) glass fibres

4. Conclusion

The use of polymer concrete as a composite material in various areas of the industry brings several advantages. However, for the maximum utilization of its positive properties in specific application cases, it is necessary to know the effect of individual components on the resulting properties of the casting. This article focused on the effect of diffused reinforcement in the form of glass and carbon fibres on compressive strength and tensile strength at bending. From the above-presented results, the use of carbon fibres in a particular polymer concrete mixture increased the compressive strength on average by about 4 MPa compared to the mixture that did not contain a diffuse reinforcement. On the other hand, the use of glass fibres causes a reduction in compressive strength compared to a non-reinforcement mixture, on average by 5 MPa. For bending tensile strength, the use of carbon fibres also has a positive effect, namely an increase in strength of about 4 MPa compared to a non-fibre reinforced blend. Glass fibres increased the tensile strength of the samples by more than 1 MPa. The hole extractions in resin indicate the presence of air bubbles in castings that have a negative effect on mechanical properties. Bubbles may be caused by insufficient vibration (compaction) of the mixture on the vibration table, or the use of too heavy a bit of resin, which was not able to run into all the cavities and fill empty spaces. The achieved results have also a practical use in industry, in the production of special CNC equipment using the created materials with the described properties.

Acknowledgement

This work was supported by the Slovak Research and Development Agency under the contract No. APVV-15-0700. This research was also supported by research grant VEGA 1/0080/20.

References

[1] Knapčíková, L. (2018). Surface topography of composite reinforced with fibres from used tyres, *Acta Tecnología,* Vol. 4, No. 2, 29-32, doi: 10.22306/atec.v4i2.36.
[2] Krolczyk, J., Legutko, S. (2014). Innovation as a key factor for entrepreneurial activity, *Applied Mechanics and Materials,* Vol. 657, 1046-1050, doi: 10.4028/www.scientific.net/AMM.657.1046.
[3] Neslušan, M., Turek, S., Brychta, J., Čep, R., Tabaček, M. (2007). *Experimental methods in splinter machining*, EDIS Žilina, Slovak Republic.
[4] Adamczak, S., Stępień, K., Wrzochal, M. (2017). Comparative study of measurement systems used to evaluate vibrations of rolling bearings, *Procedia Engineering,* Vol. 192, 971-975, doi: 10.1016/j.proeng.2017.06.167.
[5] Harničárová, M., Mitaľová, Z., Kušnerová, M., Valíček, J., Mitaľ, D., Kopal, I., Václavík, V. (2016). Analysis of physical-mechanical and surface properties of wood plastic composite materials to determine the energy balance, Defect and diffusion forum, Vol. 370, 78-89, doi: 10.4028/www.scientific.net/DDF.370.78.
[6] Krolczyk, J.B., Legutko, S. (2015). Devices and equipment for mixing granular materials in industry, *Applied Mechanics and Materials,* Vol. 809-810, 742-747, doi: 10.4028/www.scientific.net/AMM.809-810.742.
[7] Knapcíková, L., Dupláková, D., Radchenko, S., Hatala, M. (2017). Rheological behavior modelling of composite materials used in engineering industry, *TEM Journal,* Vol. 6, No. 2, 242-245, doi: 10.18421/TEM62-07.
[8] Foldyna, V., Foldyna, J., Klichova, D., Klich, J., Hlaváček, P., Bodnarova, L., Jarolim, T., Mamulová Kutláková, K. (2017). Effects of continuous and pulsating water jet on CNT/concrete composite, *Tehnički Vjesnik – Technical Gazette,* Vol. 63, No. 10, 583-589, doi: 10.5545/sv-jme.2017.4357.
[9] Agunsoye, J.O., Bello, S.A., Bello, L., Idehenre, M.M. (2016). Assessment of mechanical and wear properties of epoxy based hybrid composites, *Advances in Production Engineering & Management,* Vol. 11, No. 1, 5-14, doi: 10.14743/apem2016.1.205.
[10] Dupláková, D., Hatala, M., Duplák, J., Radchenko, S., Steranka, J. (2018). Direct metal laser sintering – Possibility of application in production process, *SAR Journal,* Vol. 1, No. 4, 123-127, doi: 10.18421/SAR14-01.
[11] Trofimov, A., Mishurova, T., Lanzoni, L., Radi, E., Bruno, G., Sevostianov, I. (2018). Microstructural analysis and mechanical properties of concrete reinforced with polymer short fibers, *International Journal of Engineering Science,* Vol. 133, 210-218, doi: 10.1016/j.ijengsci.2018.09.009.
[12] Tanyildizi, H., Asilturk, E. (2018). Performance of phosphazene-containing polymer-strengthened concrete after exposure to high temperatures, *Journal of Materials in Civil Engineering,* Vol. 30, No. 12, Article ID 04018329, doi: 10.1061/(ASCE)MT.1943-5533.0002505.
[13] Jin, N.J., Yeon, J., Min, S.-H., Yeon, K.-S. (2018). Strength developments and deformation characteristics of MMA-modified vinyl ester polymer concrete, *International Journal of Concrete Structures and Materials,* Vol. 12, Article No. 4, doi: 10.1186/s40069-018-0232-0.
[14] Şimşek, B., Uygunoğlu, T. (2018). A full factorial-based desirability function approach to investigate optimal mixture ratio of polymer concrete, *Polymer Composites,* Vol. 39, No. 9, 3199-3211, doi: 10.1002/pc.24330.
[15] Hu, B., Zhang, N.-L., Liao, Y.-T., Pan, Z.-W., Liu, Y.-P., Zhou, L.-C., Liu, Z.-J., Jiang, Z.-Y. (2018). Enhanced flexural performance of epoxy polymer concrete with short natural fibers, *Science China Technological Sciences*, Vol. 61, No. 8, 1107-1113, doi: 10.1007/s11431-017-9272-4.
[16] Li, L., Lu, J., Fang, S., Liu, F., Li, S. (2018). Flexural study of concrete beams with basalt fibre polymer bars, *Proceedings of the Institution of Civil Engineers – Structures and Buildings,* Vol. 171, No. 7, 505-516, doi: 10.1680/jstbu.16.00204.
[17] Zegardło, B., Szeląg, M., Ogrodnik, P., Bombik, A. (2018). Physico-mechanical properties and microstructure of polymer concrete with recycled glass aggregate, *Materials,* Vol. 11, No. 7, Article No. 1213, doi: 10.3390/ma11071213.
[18] Schmitt, A., Carvelli, V., Haffke, M.M., Pahn, M. (2018). Thermo-mechanical response of concrete sandwich panels reinforced with glass fiber reinforced polymer bars, *Structural Concrete,* Vol. 19, No. 3, 839-850, doi: 10.1002/suco.201700048.
[19] Niaki, M.H., Fereidoon, A., Ahangari, M.G. (2018). Effect of basalt, silica sand and fly ash on the mechanical properties of quaternary polymer concretes, *Bulletin of Materials Science,* Vol. 41, No. 3, Article No. 69, doi: 10.1007/s12034-018-1582-6.
[20] Burlacu, A., Ciocan, V., Şerbănoiu, A.A., Barbuţă, M., Verdeş, M., Cojocaru, A. (2018). Study on polymer concretes with waste of polystyrene granules, *Environmental Engineering & Management Journal*, Vol. 17, No. 5, 1229-1235, doi: 10.30638/eemj.2018.122.
[21] Niaki, M.H., Fereidoon, A., Ahangari, M.G. (2018). Experimental study on the mechanical and thermal properties of basalt fiber and nanoclay reinforced polymer concrete, *Composite Structures,* Vol. 191, 231-238, doi: 10.1016/j.compstruct.2018.02.063.
[22] Jafari, K., Tabatabaeian, M., Joshaghani, A., Ozbakkaloglu, T. (2018). Optimizing the mixture design of polymer concrete: An experimental investigation, *Construction and Building Materials,* Vol. 167, 185-196, doi: 10.1016/j.conbuildmat.2018.01.191.

[23] Niaki, M.H., Fereidoon, A., Ahangari, M.G. (2018). Mechanical properties of epoxy/basalt polymer concrete: Experimental and analytical study, *Structural Concrete,* Vol. 19, No. 2, 366-373, doi: 10.1002/suco.201700003.
[24] Hashemi, M.J., Jamshidi, M., Aghdam, J.H. (2018). Investigating fracture mechanics and flexural properties of unsaturated polyester polymer concrete (UP-PC), *Construction and Building Materials,* Vol. 163, 767-775, doi: 10.1016/j.conbuildmat.2017.12.115.
[25] Lu, Y., Zhu, T., Li, S., Liu, Z. (2018). Bond behavior of wet-bonded carbon fiber-reinforced polymer-concrete interface subjected to moisture, *International Journal of Polymer Science,* Vol. 2018, Article ID 3120545, doi: 10.1155/2018/3120545.
[26] Şimşek, B., Uygunoğlu, T. (2017). A design of experiment application to improve raw materials utilization ratio of polymer concrete composites, *Journal of Engineering Research,* Vol. 5, No. 4., 1-18.
[27] Jafari, K., Toufigh, V. (2017). Experimental and analytical evaluation of rubberized polymer concrete, *Construction and Building Materials,* Vol. 155, 495-510, doi: 10.1016/j.conbuildmat.2017.08.097.
[28] Shokrieh, M.M., Rezvani, S., Mosalmani, R. (2017). Mechanical behavior of polyester polymer concrete under low strain rate loading conditions, *Polymer Testing,* Vol. 63, 596-604, doi: 10.1016/j.polymertesting.2017.09.015.
[29] Hwang, E.-H., Kim, Y.-Y., Song, M.-K. (2017). Durability of high performance polymer concrete composites (focusing on chemical resistance and hot water resistance), *Applied Chemistry for Engineering*, Vol. 28, No. 3, 360-368, doi: 10.14478/ACE.2017.1040.
[30] Yue, Q., Liu, Z., Li, R., Chen, X. (2017). Experimental investigation into the development length of carbon-fiber-reinforced polymer grids in concrete, *Advances in Structural Engineering,* Vol. 20, No. 6, 953-962, doi: 10.1177/1369433216668360.
[31] Agunsoye, J.O., Bello, S.A., Bello, L., Idehenre, M.M. (2016). Assessment of mechanical and wear properties of epoxy-based hybrid composites, *Advances in Production Engineering & Management,* Vol. 11, No. 1, 5-14, doi: 10.14743/apem2016.1.205.